Inorg. Chem. **2003**, *42*, 3086–3096

Complexation of Diphenyl(phenylacetenyl)phosphine to Rhodium(III) Tetraphenyl Porphyrins: Synthesis and Structural, Spectroscopic, and Thermodynamic Studies

Eugen Stulz,*,† Sonya M. Scott, Andrew D. Bond, Sijbren Otto, and Jeremy K. M. Sanders*

University Chemical Laboratory, University of Cambridge, Lensfield Road, Cambridge CB2 1EW, U.K.

Received December 11, 2002

The coordination of diphenyl(phenylacetenyl)phosphine (DPAP, **1**) to (X)Rh^{III}TPP (X = I (**2**) or Me (**3**); TPP = tetraphenyl porphyrin) was studied in solution and in the solid state. The iodide is readily displaced by the phosphine, leading to the bis-phosphine complex [(DPAP)$_2$Rh(TPP)](I) (**4**). The methylide on rhodium in **3** is not displaced, leading selectively to the mono-phosphine complex (DPAP)(Me)Rh(TPP) (**5**). The first and second association constants, as determined by isothermal titration calorimetry and UV–vis titrations, are in the range 10^4–10^7 M^{-1} (in CH_2Cl_2). Using LDI-TOF mass spectrometry, the mono-phosphine complexes can be detected but not the bis-phosphine complexes. The electronic spectrum of **4** is similar to those previously reported with other tertiary phosphine ligands, whereas (DPAP)(I)Rh(TPP) (**6**) displays a low energy B-band absorption and a high energy Q-band absorption. In contrast to earlier reports, displacement of the methylide on rhodium in **5** could not be observed at any concentration, and the electronic spectra of **4** and **5** are almost identical. Isothermal titration calorimetry experiments showed that all binding events are exothermic, and all are enthalpy driven. The largest values of ΔG° are found for **6**. The thermodynamic and UV–vis data reveal that the methylide and the phosphine ligand have an almost identical electronic *trans*-influence on the sixth ligand.

Introduction

Rhodium(III) porphyrin complexes are of interest because of their ability to act as hydrogen activators in hydride transfer reactions[1,2] and as catalysts in hydrogen evolution.[3] A variety of applications, where Rh(II) porphyrins act as redox-activators of C−H bonds, have also been reported.[4−6] In bioinorganic chemistry, rhodium(III) porphyrins have been used for biomimetic studies on vitamin B_{12}[7] and on cytochrome *c*.[8] The redox chemistry and photophysical properties of Rh porphyrins have extensively been investigated by James,[9] Kadish,[4,10−13] Collman,[1,8,14] Wayland,[2,6,7] and Savéant.[3,15] It thus seems promising to embed rhodium(III) porphyrins into multiporphyrin arrays to obtain constructs where the rhodium porphyrin could act as a redox or as a

* To whom correspondence should be addressed. E-mail: Eugen.Stulz@unibas.ch (E.S.); jkms@cam.ac.uk (J.K.M.S.).

† Present address: Department of Chemistry, University of Basel, St. Johanns-Ring 19, 4056 Basel, Switzerland.

(1) Collman, J. P.; Ha, Y.; Guilard, R. *Inorg. Chem.* **1993**, *32*, 1788.
(2) Bosch, H. W.; Wayland, B. B. *J. Chem. Soc., Chem. Commun.* **1986**, 900.
(3) Grass, V.; Lexa, D.; Savéant, J. M. *J. Am. Chem. Soc.* **1997**, *119*, 7526.
(4) Guilard, R.; Kadish, K. M. *Chem. Rev.* **1988**, *88*, 1121.
(5) Nelson, A. P.; DiMagno, S. G. *J. Am. Chem. Soc.* **2000**, *122*, 8569.
(6) (a) Wayland, B. B.; Sherry, A. E.; Bunn, A. G. *J. Am. Chem. Soc.* **1993**, *115*, 7675. (b) Wayland, B. B.; Ba, S.; Sherry, A. E. *J. Am. Chem. Soc.* **1991**, *113*, 5305. (c) Zhang, X. X.; Wayland, B. B. *J. Am. Chem. Soc.* **1994**, *116*, 7897. (d) Zhang, X. X.; Parks, G. F.; Wayland, B. B. *J. Am. Chem. Soc.* **1997**, *119*, 7938. (e) Basickes, L.; Bunn, A. G.; Wayland, B. B. *Can. J. Chem.* **2001**, *79*, 854. (f) Barrett, A. G. M.; Braddock, D. C.; Lenoir, I.; Tone, H. *J. Org. Chem.* **2001**, *66*, 8260. (g) Kimata, S.; Aida, T. *Tetrahedron Lett.* **2001**, *42*, 4187. (h) Lo Schiavo, S.; Serroni, S.; Puntoriero, F.; Tresoldi, G.; Piraino, P. *Eur. J. Inorg. Chem.* **2002**, 79. (i) Tagliatesta, P.; Pastorini, A. *J. Mol. Catal. A: Chem.* **2002**, *185*, 127. (j) Mak, K. W.; Yeung, S. K.; Chan, K. S. *Organometallics* **2002**, *21*, 2362.
(7) Wayland, B. B.; Vanvoorhees, S. L.; Delrossi, K. J. *J. Am. Chem. Soc.* **1987**, *109*, 6513.
(8) Collman, J. P.; Boulatov, R. *J. Am. Chem. Soc.* **2000**, *122*, 11812.
(9) Thackray, D. C.; Ariel, S.; Leung, T. W.; Menon, K.; James, B. R.; Trotter, J. *Can. J. Chem.* **1986**, *64*, 2440.
(10) Anderson, J. E.; Yao, C.-L.; Kadish, K. M. *Inorg. Chem.* **1986**, *25*, 3224.
(11) Anderson, J. E.; Yao, C.-L.; Kadish, K. M. *Inorg. Chem.* **1986**, *25*, 718.
(12) Kadish, K. M.; Araullo, C.; Yao, C.-L. *Organometallics* **1988**, *7*, 1583.
(13) Kadish, K. M.; Hu, Y.; Boschi, T.; Tagliatesta, P. *Inorg. Chem.* **1993**, *32*, 2996.
(14) Collman, J. P.; Ha, Y. Y.; Guilard, R.; Lopez, M. A. *Inorg. Chem.* **1993**, *32*, 1788.

10.1021/ic026257a CCC: $25.00
Published on Web 04/01/2003

Chart 1

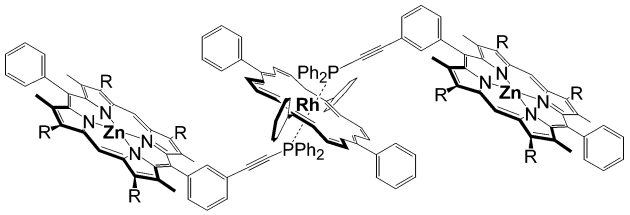

[**Zn**/**Rh**/**Zn**], R = hexyl

photophysically active center.[16] In previous work, we have introduced Rh(III) porphyrins into supramolecular arrays[17] and studied a variety of N-, S-, and Se-coordination compounds both in solution and in the solid state,[18] culminating in the formation of a heterometallic porphyrin undecamer.[19] Recently, we have used the coordination of a phosphine substituted porphyrin to Rh^{III}(TPP) to prepare selectively a cyclic porphyrin tetramer by amplification from a biased dynamic combinatorial library[20] using 4,4′-bipyridine as scaffold.[21]

Alkynyl substituted porphyrins provide versatile building blocks for the construction of supramolecular assemblies.[22] Attachment of a diphenyl phosphine group to porphyrins via an acetylenic linker provides a simple route to phosphine substituted porphyrins,[23] which are ideal building blocks for the construction of heterometallic porphyrin arrays. In order to be able to predict electronic interactions in arrays such as a [Zn/Rh/Zn] trimer (Chart 1), it is essential to have basic knowledge about the structure and physical properties of phosphorus rhodium porphyrin complexes. We have previously used diphenyl(phenylacetenyl)phosphine (DPAP, Chart 2) (**1**) to study the physical properties of phosphine complexes of a ruthenium porphyrin.[24,25] This phosphine ligand serves as a model to mimic the substitution pattern in our phosphine substituted porphyrins.

Chart 2

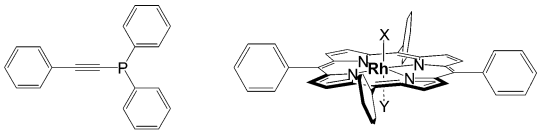

DPAP (**1**)

X	Y	
I	MeOH	(**2**)
Me	-	(**3**)
DPAP	DPAP	(**4**)
Me	DPAP	(**5**)
I	DPAP	(**6**)

Here, we present a detailed study on the affinity of DPAP (**1**) toward (X)(Y)Rh^{III}(TPP) [X = I, Y = MeOH (**2**); X = Me (**3**), Chart 2].[26] The porphyrins have been chosen on the basis that we already have demonstrated that they form bis-phosphine complexes with **2**;[21] the methylide in **3** is thought to be an inert ligand, blocking the sixth coordination site so that mono-phosphine complexes can selectively be obtained. All complexes have been studied in solution using ^{1}H NMR and $^{31}P\{^1H\}$ NMR spectroscopy, UV−vis spectroscopy, mass spectrometry, and isothermal titration calorimetry (ITC). We also report on the solid-state structures of **2**, **3**, [$(DPAP)_2Rh^{III}$(TPP)](I) (**4**), and (DPAP)(Me)Rh^{III}(TPP) (**5**).

Experimental Section

General. Methylene chloride (CH_2Cl_2), chloroform ($CHCl_3$), and methanol (MeOH) were obtained from Bamford Laboratories (U.K.) and used as received; $CDCl_3$ (euriso-top, France) was filtered over basic alumina prior to use. $^tBu_4NI$ (Aldrich) was used as purchased. DPAP (**1**), (MeOH)(I)Rh(TPP) (**2**), and (Me)Rh(TPP) (**3**) were prepared according to literature procedures.[27] NMR spectra were recorded on a Bruker DPX400 NMR spectrometer at 161.98 MHz ($^{31}P\{^1H\}$, H_3PO_4 external standard), or on a Bruker DRX500 NMR spectrometer at 500.13 MHz (^{1}H). Abbreviations for NMR spectra used are the following: s, singlet; d, doublet; dd, doublet of doublets; t, triplet; dt, doublet of triplets; q, quartet; m, multiplet. UV−vis spectra were recorded on a Varian Cary 100 Bio spectrophotometer. LDI-TOF mass spectra were recorded on a Kompact MALDI 4 mass spectrometer (Kratos Analytical Ltd), operated in the linear positive mode, and using neat samples. Isothermal titration calorimetry (ITC) was performed on a MICROCAL. INC microcalorimeter at 25 °C.

UV−vis titrations were performed at the following concentrations: [**2**] = 10^{-4} M ([**1**] = 10^{-3} M), [**2**] = 10^{-5} M ([**1**] = 10^{-3} M), [**2**] = 10^{-6} M ([**1**] = 10^{-4} M); [**3**] = 5×10^{-4} M ([**1**] = 10^{-2} M), [**3**] = 10^{-4} M ([**1**] = 10^{-2} M), [**3**] = 10^{-5} M ([**1**] = 10^{-3} M), [**3**] = 10^{-6} M ([**1**] = 10^{-5} M). Solutions were prepared from stock solutions ([**2**] = 10^{-3} M, [**3**] = 10^{-3} M, [**1**] = 10^{-2} M) in $CHCl_3$.

(15) Grass, V.; Lexa, D.; Momenteau, M.; Savéant, J. M. *J. Am. Chem. Soc.* **1997**, *119*, 3536.
(16) Vitols, S. E.; Friesen, D. A.; Williams, D. S.; Melamed, D.; Spiro, T. G. *J. Phys. Chem.* **1996**, *100*, 207.
(17) Kim, H. J.; Redman, J. E.; Nakash, M.; Feeder, N.; Teat, S. J.; Sanders, J. K. M. *Inorg. Chem.* **1999**, *38*, 5178.
(18) Redman, J. E.; Feeder, N.; Teat, S. J.; Sanders, J. K. M. *Inorg. Chem.* **2001**, *40*, 3217.
(19) Redman, J. E.; Feeder, N.; Teat, S. J.; Sanders, J. K. M. *Inorg. Chem.* **2001**, *40*, 2486.
(20) (a) Otto, S.; Furlan, R. L. E.; Sanders, J. K. M. *Science* **2002**, *297*, 590. (b) Roberts, S. L.; Furlan, R. L. E.; Cousins, G. R. L.; Sanders, J. K. M. *Chem. Commun.* **2002**, 938. (c) Furlan, R. L. E.; Ng, Y. F.; Otto, S.; Sanders, J. K. M. *J. Am. Chem. Soc.* **2001**, *123*, 8876. (d) Furlan, R. L. E.; Ng, Y. F.; Cousins, G. R. L.; Redman, J. E.; Sanders, J. K. M. *Tetrahedron* **2002**, *58*, 771.
(21) Stulz, E.; Ng, Y.-F.; Scott, S. M.; Sanders, J. K. M. *Chem. Commun.* **2002**, 524.
(22) (a) Mak, C. C.; Bampos, N.; Darling, S. L.; Montalti, M.; Prodi, L.; Sanders, J. K. M. *J. Org. Chem.* **2001**, *66*, 4476. (b) Webb, S. J.; Sanders, J. K. M. *Inorg. Chem.* **2000**, *39*, 5912. (c) Webb, S. J.; Sanders, J. K. M. *Inorg. Chem.* **2000**, *39*, 5920. (d) Nakash, M.; Sanders, J. K. M. *J. Chem. Soc., Perkin Trans. 2* **2001**, 2189. (e) Mak, C. C.; Pomeranc, D.; Montalti, M.; Prodi, L.; Sanders, J. K. M. *Chem. Commun.* **1999**, 1083. (f) Kim, H. J.; Bampos, N.; Sanders, J. K. M. *J. Am. Chem. Soc.* **1999**, *121*, 8120. (g) Wilson, G. S.; Anderson, H. L. *Chem. Commun.* **1999**, 1539. (h) Taylor, P. N.; Anderson, H. L. *J. Am. Chem. Soc.* **1999**, *121*, 11538. (i) Kodis, G.; Liddell, P. A.; de la Garza, L.; Clausen, C.; Lindsey, J. L.; Moore, A. L.; Moore, T. A.; Gust, D. *J. Phys. Chem. A* **2002**, *106*, 2036. (j) Ambroise, A.; Kirmaier, C.; Wagner, R. W.; Loewe, R. S.; Bocian, D. F.; Holten, D.; Lindsey, J. L. *J. Org. Chem.* **2002**, *67*, 3811. (k) Fletcher, J. T.; Therien, M. J. *Inorg. Chem.* **2002**, *41*, 331. (l) Shediac, R.; Gray, M. H. B.; Uyeda, H. T.; Johnson, R. C.; Hupp, J. T.; Angiolillo, P. J.; Therien, M. J. *J. Am. Chem. Soc.* **2000**, *122*, 7017.
(23) Darling, S. L.; Stulz, E.; Feeder, N.; Bampos, N.; Sanders, J. K. M. *New J. Chem.* **2000**, *24*, 261.
(24) Stulz, E.; Sanders, J. K. M.; Montalti, M.; Prodi, L.; Zaccheroni, N.; de Biani, F.; Grigiotti, E.; Zanello, P. *Inorg. Chem.* **2002**, *41*, 5269.
(25) Stulz, E.; Maue, M.; Feeder, N.; Teat, S. J.; Ng, Y. F.; Bond, A. D.; Darling, S.; Sanders, J. K. M. *Inorg. Chem.* **2002**, *41*, 5255.
(26) On crystallization from CH_2Cl_2−MeOH, **2** always carries methanol as a sixth ligand, which can be detected in the ^{1}H NMR spectrum; in **3**, no additional bound solvent could be detected. See ref 19.
(27) DPAP: Carty, A. J.; Hota, N. K.; Ng, T. W.; Patel, H. A.; O'Connor, T. J. *Can. J. Chem.* **1971**, *49*, 2706. **2**, **3**: Kim, H.-J.; Bampos, N.; Sanders, J. K. M. *J. Am. Chem. Soc.* **1999**, *121*, 8120.

Table 1. Crystallographic Data for (MeOH)(I)Rh(TPP) (**2**), (Me)Rh(TPP) (**3**), [(dpap)$_2$Rh(TPP)](I) (**4**), and (dpap)(Me)Rh(TPP) (**5**)

	2·$CHCl_3$	**3**	**4**·$2CHCl_3$	**5**
formula	$C_{46}H_{33}Cl_3IN_4ORh$	$C_{45}H_{31}N_4Rh$	$C_{86}H_{60}Cl_6IN_4P_2Rh$	$C_{65}H_{46}N_4PRh$
M	993.92	730.65	1653.83	1016.94
T/K	180(2)	180(2)	180(2)	180(2)
radiation, λ/Å	Mo Kα, 0.707	Mo Kα, 0.707	Mo Kα, 0.707	Mo Kα, 0.707
cryst syst	triclinic	tetragonal	monoclinic	triclinic
space group	$P\bar{1}$	$I4/m$	$C2/c$	$P\bar{1}$
a/Å	9.7114(5)	13.4741(5)	25.9530(6)	13.3949(7)
b/Å	11.1479(7)	13.4741(5)	11.6120(2)	13.3979(8)
c/Å	21.6504(13)	9.6462(5)	23.8501(6)	14.1945(9)
α/deg	80.451(3)	90	90	83.942(3)
β/deg	89.804(3)	90	91.116(1)	86.237(3)
γ/deg	65.549(3)	90	90	89.875(4)
V/Å^3	2098.6(2)	1751.28(13)	7186.3(3)	2527.7(3)
Z	2	2	4	2
ρ_{calcd}/g cm^{-3}	1.573	1.386	1.529	1.336
μ/mm^{-1}	1.374	0.526	0.986	0.416
θ_{max}/deg	25.02	24.68	25.01	21.97
total data	18266	3796	20541	15705
unique data	7318	802	6306	6127
R_{int}	0.0673	0.0739	0.0408	0.0815
R1 [$F^2 > 2\sigma(F^2)$]	0.0706	0.0408	0.0345	0.1134
wR2 (all data)	0.1841	0.0753	0.0828	0.2873
S	1.07	1.15	1.04	1.10

ITC experiments were done at the following concentrations ($CHCl_3$, 298 K): [**2**] = 2×10^{-5} M, [**1**] = 4×10^{-4} M; [**3**] = 10^{-3} M, [**1**] = 10^{-2} M. For the ITC experiment in the presence of additional iodide, both solutions of **1** (4×10^{-4} M) and **2** (2×10^{-5} M) contained 10^{-4} M ^{t}Bu$_4$NI. ^{1}H NMR titrations of **3** with **1** were performed in degassed (Ar saturated) $CDCl_3$ at [**3**] = 5×10^{-4} M, using [**1**] = 10^{-2} M.

X-ray diffraction data were collected using a Nonius Kappa CCD diffractometer. Structures were solved by direct methods using either *SHELXS*-97[28] or *SIR*-92[29] and refined against all F^2 data using *SHELXL*-97.[28] A summary of the crystallographic data is given in Table 1.

[(DPAP)$_2$Rh(TPP)](I) (4). Compound **2** (50.0 mg, 59 mmol) was dissolved in $CHCl_3$ (7 mL), and solid **1** (42.3 mg, 148 mmol) was added. Once all the starting material had dissolved, the solvent was evaporated, and the residues were dissolved in hot $CHCl_3$ (1.5 mL). After careful layering of methanol (15 mL), the mixture was left to crystallize overnight. The product was filtered off, washed with methanol, and dried in vacuo. The product was obtained as dark-orange crystals (71.4 mg, 55 mmol, 94%, calcd for $C_{84}H_{58}I_1N_4P_2Rh_1$). Crystals suitable for X-ray analysis were grown from a concentrated $CHCl_3$ solution (200 μL) of **4**, layered with methanol (500 μL). UV−vis ($CHCl_3$, 298 K): λ (log ϵ) 323 (4.63), 357 (4.56), 376 (shoulder), 445 (5.28), 557 (4.23), 596 (4.19). ^{1}H NMR (500.13 MHz, $CDCl_3$, 300 K): δ 4.12 [q, ^1J = 7.1 Hz, 8H, *o*-H of P(Ph)$_2$], 6.58 [dt, ^1J_o = 7.9 Hz, ^1J_m = 1.5 Hz, 8H, *m*-H of P(Ph)$_2$], 6.89 (dd, ^1J_o = 8.3 Hz, ^1J_m = 1.4 Hz, 4H, *o*-H of C≡C−PPh), 6.94 [t, ^1J = 10.8 Hz, 8H, *p*-H of P(Ph)$_2$], 7.28 (m, 4H, *m*-H of C≡C−PPh), 7.35 (m, 2H, *p*-H of C≡C−PPh), 7.62 (m, 12H, *m*,*p*-H of *meso*-Ph), 7.67 (m, 8H, *o*-H of *meso*-Ph), 8.79 (s, 8H, β-pyrrole). ^{31}P NMR (161.98 MHz, $CDCl_3$, 300 K): δ −10.1 ppm (d, $^1J_{Rh,P}$ = 87 Hz). LDI-TOF MS: *m*/*z* 1002.0, 716.4.

(DPAP)(Me)Rh(TPP) (5). Compound **3** (12.0 mg, 16 mmol) was dissolved in $CHCl_3$ (4 mL), and solid **1** (5.9 mg, 20.5 mmol) was added. Once all the starting material had dissolved (2−3 min), the solvent was evaporated, and the residues were crystallized from $CHCl_3$−methanol (1.0 + 8.0 mL). The product was filtered off, washed with methanol, and dried in vacuo to give **5** as a dark-orange powder (15.0 mg, 14.7 mmol, 92%, calcd for $C_{65}H_{46}N_4P_1Rh_1$). Crystals suitable for X-ray analysis were grown from a concentrated $CHCl_3$ solution (200 μL) of **5**, layered with methanol (500 μL). UV−vis ($CHCl_3$, 298 K): λ (log ϵ) 356 (3.62), 418 (shoulder), 444 (5.22), 516 (3.85), 556 (4.09), 597 (4.10), 620 (3.62). ^{1}H NMR (400.13 MHz, $CDCl_3$, 300 K): δ −6.52 ppm (d, ^1J = 2.56 Hz), 4.51 [t, ^1J = 8.3 Hz, 4H, *o*-H of P(Ph)$_2$], 6.58 [dt, ^1J_o = 9.8 Hz, ^1J_m = 2.0 Hz, 4H, *m*-H of P(Ph)$_2$], 6.56 [dt, ^1J_o = 8.4 Hz, ^1J_m = 1.1 Hz, 2H, *p*-H of P(Ph)$_2$], 7.06 (dd, ^1J_o = 7.0 Hz, ^1J_m = 1.3 Hz, 2H, *o*-H of C≡C−PPh), 7.19 (m, 1H, *p*-H of C≡C−PPh), 7.24 (m, 2H, *m*-H of C≡C−PPh), 7.62 (m, 4H, *m*-H of *meso*-Ph), 7.68 (m, 8H, *m*,*p*-H of *meso*-Ph), 7.71 (dt, ^1J_o = 7.0 Hz, ^1J_m = 1.5 Hz, 4H, *o*-H of *meso*-Ph), 8.19 (dt, ^1J_o = 6.9 Hz, ^1J_m = 1.5 Hz, 4H, *o*-H of *meso*-Ph), 8.58 (s, 8H, β-pyrrole). ^{31}P NMR (161.98 MHz, $CDCl_3$, 300 K): δ −28 ppm. LDI-TOF MS: *m*/*z* 1032.4, 1018.2, 1002.0, 745.6, 730.7, 715.7.

Results and Discussion

Synthesis and NMR Spectroscopy of (DPAP)$_2$Rh^{III}TPP. Addition of 1 equiv of DPAP (**1**) to (MeOH)(I)Rh(TPP) (**2**) in $CDCl_3$ did not lead to clean formation of (DPAP)(I)Rh(TPP) (**6**).[9] Instead, a mixture of both mono- and bis-phosphine complexes was obtained, as judged from the phosphorus NMR spectrum (Figure 1a). Two distinct doublets at δ −9.5 ppm ($^1J_{Rh,P}$ = 114 Hz) and at δ −10.1 ppm ($^1J_{Rh,P}$ = 87 Hz) were observed, whereas unbound **1** shows a singlet at δ −32 ppm (not shown). The overall downfield shift of the phosphorus nucleus on complexation to rhodium can be rationalized in terms of electron donation of the ligand to the Lewis acidic metal center upon σ-bond formation, which outweighs the porphyrin ring current induced upfield shift.[25] The iodide is readily displaced by **1**, in contrast to the displacement of chloride by PPh_3 and PEt_3 on rhodium porphyrins, which requires a large excess of phosphine.[9] Addition of a second equivalent of **1** at ambient temperature transforms the mixture within minutes to [(DPAP)$_2$Rh(TPP)](I) (**4**), (δ −10.1 ppm, $^1J_{Rh,P}$ = 87 Hz, Figure 1b). This allows the mono- and the bis-phosphine complex to be distinguished

(28) Sheldrick, G. M. *SHELXS-97*; University of Göttingen: Göttingen, Germany, 1997.
(29) Altomare, A.; Cascarano, G.; Giacovazzo, C.; Guagliardi, A.; Burla, M. C.; Polidori, G.; Camalli, M. *J. Appl. Crystallogr.* **1994**, *27*, 435.

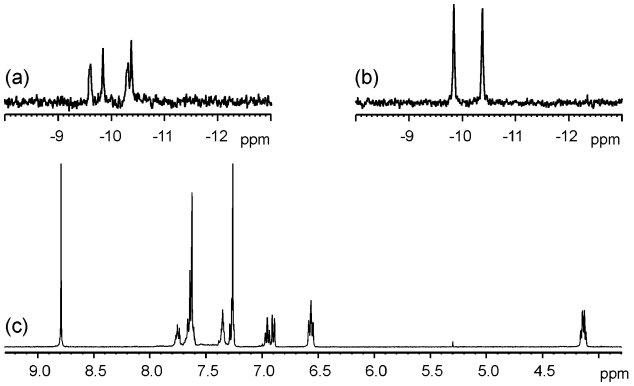

Figure 1. (a) $^{31}P\{^1H\}$ NMR spectrum of a 1:1 mixture of **2** and **1**; (b) $^{31}P\{^1H\}$ NMR spectrum of **4**; (c) part of the ^1H NMR spectrum of **4**. Spectra are recorded in $CDCl_3$ (500 MHz for ^1H, 162 MHz for ^{31}P) at 300 K, c = 10 mM.

on the basis of both the $^{31}P\{^1H\}$ NMR chemical shift and the $^1J_{Rh,P}$ coupling constant. The coupling constants, but not the chemical shifts, are very close to those found in PPh_3 complexes of Rh^{III}(OEP), where $^1J_{Rh,P}$ = 124 Hz (δ −2.6 ppm) and 86 Hz (δ 9.5 ppm) for the bis- and mono-phosphine complex, respectively.[9] Also, the observed $^{31}P\{^1H\}$ NMR chemical shifts contrast with analogous ruthenium(II) porphyrin−DPAP complexes, where the mono-phosphine complex (δ −12 ppm) and bis-phosphine complex (δ +3 ppm) show a chemical shift difference of $\Delta\delta$ = +15 ppm.[25] In the Rh(III) binding, the bis-phosphine complexes resonate at a slightly higher field than the mono-phosphine complexes, whereas in the Ru(II) complexes, the order is reversed. This can be attributed to a different *trans*-influence of the iodide on rhodium compared to the strong π-acceptor properties of the carbonyl on ruthenium.

The proton signals of the phenyl phosphorus substituents are shifted upfield due to the proximity to the shielding region of the aromatic porphyrin core (Figure 1c) and confirm binding of **1** to the porphyrin central metal. Complex **4** can easily be obtained in pure form by mixing a slight excess of **1** with **2** in CH_2Cl_2 or $CHCl_3$, and crystallizing from a layered $CHCl_3$−methanol system.

Synthesis and NMR Spectroscopy of (DPAP)(Me)Rh^{III}(TPP). (Me)RhTPP (**3**) selectively forms the mono-phosphine adduct (DPAP)(Me)Rh(TPP) (**5**) in solution (Figure 2a) and can be isolated in an analogous way to **4**. The resonance for the σ-bonded methylide in **5** appears as a broadened signal at low concentrations ([**5**] < 10^{-3} M). Its chemical shift is concentration dependent, indicating dynamic ligand binding of **1** to **5**. The limiting value at high concentration ([**5**] > 10 mM), or upon addition of excess ligand (0.1 mM **3**, 10 mM **1**), is at δ −6.52 ppm. The inset in Figure 2a shows the gradual upfield shift of the signal from the Rh−CH_3 group upon titrating **1** with **3**. The final value displays a significant upfield shift compared to that of the parent (Me)RhTPP (**3**) (δ −5.80 ppm). The chemical shift difference in **5** (compared to **3**) is much larger than in the analogous PPh_3 complex in C_6D_6 ($\Delta\delta$ = 0.40 ppm),[12] where the value for the (PPh_3)(Me)RhTPP complex is δ −5.94 ppm, indicated as a multiplet. The downfield shift indicates a larger electron density on the methylide due to the σ-donation of **1**

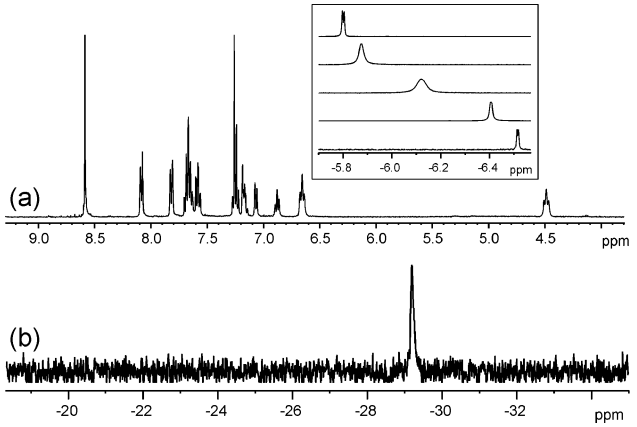

Figure 2. (a) ^1H NMR spectrum of **5**; the inset shows, from top to bottom, the gradually upfield shifted resonance of the methylide signal after addition of 0, 0.2, 0.6, 0.9, and 1.5 equiv of **1** at [**3**] = 5 mM; (b) $^{31}P\{^1H\}$ NMR spectrum of **5**. Conditions are as indicated in Figure 1.

and reveals a strong *trans*-influence of **1**; just such a *trans*-influence of phosphines was previously detected using the Rh−C Raman frequencies in (Me)Rh(TTP) phosphine complexes[30] and agrees with our NMR results.

In the presence of excess **1**, the *o*-proton signal of the phosphorus phenyl substituent at δ 4.49 ppm becomes broadened and downfield shifted, which shows that fast ligand exchange occurs. The two different ligands on the central metal render the α- and β-sides of the porphyrin nonequivalent, which is expressed in the splitting of the *meso*-phenyl proton resonances; i.e., the *o*-protons appear at δ 7.82 and 8.09 ppm. The $^{31}P\{^1H\}$ NMR of **5** is distinctively different with the resonance for the bound phosphorus at δ −29 ppm as a broadened signal, and no $^1J_{Rh,P}$ coupling can be detected (Figure 2b). The marginal shift, the broadening, and the lack of a coupling to rhodium arises from a dynamic exchange of unbound and bound ligand.

Solid-State Structures. Single crystals of rhodium porphyrins **2**−**5** suitable for X-ray analysis were grown from concentrated $CHCl_3$ solutions layered with methanol. The molecular units are shown in Figure 3, and selected geometrical data are summarized in Table 2. The crystals of **2** contain additional solvent molecules (one $CHCl_3$ per porphyrin complex). The *meso*-phenyl substituent at C5 displays disorder which was modeled in two orientations of equal occupancy, with the phenyl rings constrained to be regular hexagons and a single displacement parameter common to all C atoms. Porphyrin **3** crystallizes in space group *I*4/*m* with the complex positioned on a site of 4/*m* symmetry, such that it displays gross D_{4h} point symmetry. The methylide carbon atom could be distinguished as 50% occupied on the basis of its displacement parameter, but no other ligand could be located on rhodium. Thus, rhodium is 5-coordinate with the methylide carbon disordered equally above and below the porphyrin plane.[31] Porphyrin **3**, together with previously reported analogous structures,[5,17,32] shows that rhodium(III) porphyrins bearing a methylide ligand generally remain 5-coordinate. The Rh−C bond length for **3** (1.968(12) Å) is

(30) Huang, J. K.; Haar, C. M.; Nolan, S. P.; Marshall, W. J.; Moloy, K. G. *J. Am. Chem. Soc.* **1998**, *120*, 7806.

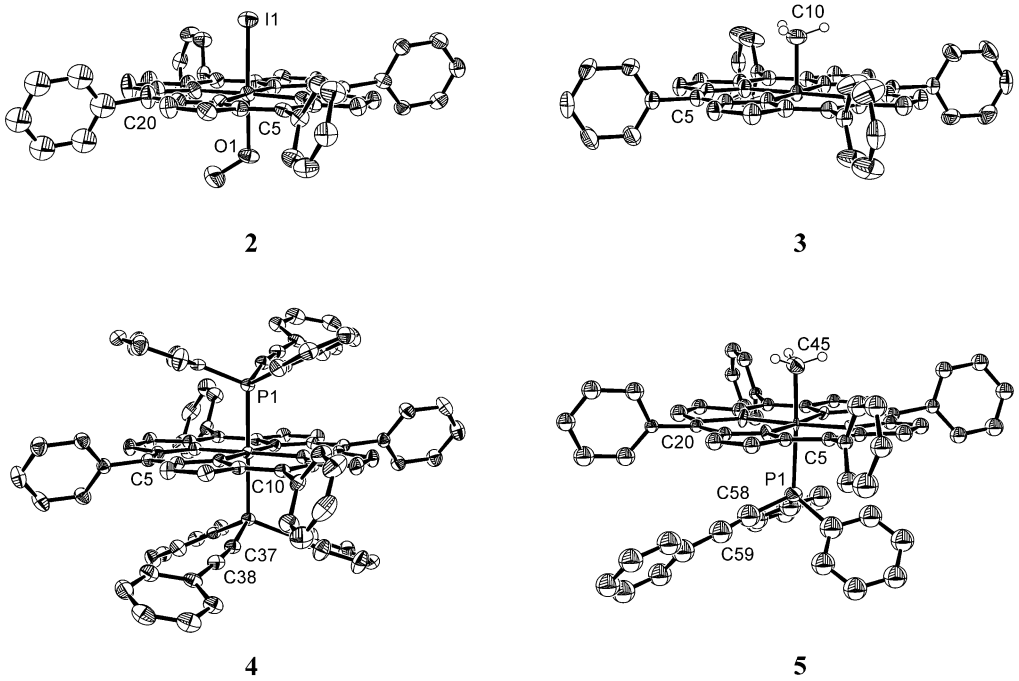

2 **3** **4** **5**

Figure 3. Molecular units of (MeOH)(I)Rh(TPP) (**2**), (Me)Rh(TPP) (**3**), $(DPAP)_2$(Rh)(TPP) (**4**), and (DPAP)(Me)Rh(TPP) (**5**), showing displacement ellipsoids at 50% probability. H atoms (except on the rhodium bound methyl carbon C10 in **3** and C45 in **5**) and the iodide counterion in **4** have been omitted for clarity. In **5**, only one of the two orientations of the disordered DPAP moiety is shown.

Table 2. Selected Geometrical Data for **2**−**5** (Å, deg)

	2·$CHCl_3$	**3**	**4**·$2CHCl_3$	**5**
σ/deg[a]	0.029	0	0.034	0.043
β/deg[b]	87.1		88.9	89.6
α/deg[b]	89.8	90	88.9	87.3
Rh−L2/Å	2.210(6) (O1)		2.3707(7) (P1′)	2.059(11) (C45)
Rh−L1/Å	2.5719(8) (I1)	1.968(12) (C10)	2.3707(7) (P1)	2.512(3) (P1)
Rh−N4/Å	2.028(7)	2.018(3)	2.043(2)	2.033(6)
Rh−N3/Å	2.026(7)	2.018(3)	2.041(2)	2.024(6)
Rh−N2/Å	2.028(7)	2.018(3)	2.043(2)	2.032(6)
Rh−N1/Å	2.025(7)	2.018(3)	2.041(2)	2.028(7)
dihedral angles of	73.0 (C5−Ph)	90	61.2 (C5−Ph)	79.9 (C5−Ph)
phenyl groups with	84.7 (C5−Ph′)		66.8 (C10−Ph)	77.7 (C10−Ph)
porphyrin plane/deg	71.2 (C10−Ph)			78.6 (C15−Ph)
	75.5 (C15−Ph)			75.4 (C20−Ph)
	82.7 (C20−Ph)			
deviation of *ipso*	−0.21 (C21)	0	0.17 (C11)	0.20 (C21)
carbons	0.32 (C21′)		−0.17 (C17)	0.17 (C27)
perpendicular to	−0.06 (C27)		0.17 (C11′)	0.17 (C33)
porphyrin plane/Å	0.26 (C33)		−0.17 (C17′)	0.22 (C39)
	0.04 (C39)			

[a] σ denotes the average perpendicular deviation of the porphyrin core atoms from the least-squares plane through all 24 core atoms. [b] α and β denote the angle formed by the Rh−L1/L2 bond with the least-squares porphyrin plane.

slightly shorter than in $CH_3Rh(F_{28}TPP)$ (2.027(4) Å),[5] in $CH_3Rh(OEP)$ (2.031(6) Å),[32b] or in $CH_3Rh(OETAP)$ (2.034(7) Å).[32c] Complex **4** crystallizes in space group *C*2/*c* with two $CHCl_3$ molecules per porphyrin complex. The complex is sited on a center of symmetry (point symmetry C_i). The crystals of **5** were small and relatively weakly diffracting, and data were observed only to $2\theta = 22°$ (Mo Kα radiation; equivalent to 0.95 Å resolution). In this case, anisotropic refinement was possible only for the heavy atoms (Rh, P), the porphyrin core, and the methylide carbon atom. The DPAP ligand is disordered and was modeled in two orientations of equal occupancy related by rotation about the Rh−P bond, with the phenyl rings constrained to be regular hexagons.

In all these structures, the Rh−N bond distances lie in the expected range 2.018−2.043 Å. The overall deviations

(31) The single-crystal structure of $Zn(TPP)(H_2O)$ displays a notable example of this type of disorder. In an early structure report, the disorder of the water molecule led to the incorrect description of the structure as a dihydrate containing 6-coordinate Zn: Fleischer, E. B.; Miller, C. K.; Webb, L. E. *J. Am. Chem. Soc.* **1964**, *86*, 2342. The correct disordered interpretation was distinguished later on the basis of the displacement parameter of the oxygen atom: Glick, M. D.; Cohen, G. H.; Hoard, J. L. *J. Am. Chem. Soc.* **1967**, *89*, 1996.

(32) (a) Whang, D. M.; Kim, K. M. *Acta Crystallogr., Sect. C: Cryst. Struct. Commun.* **1991**, *47*, 2547. (b) Takenaka, A.; Syal, S. K.; Sasada, Y.; Omura, T.; Ogoshi, H.; Yoshida, Z.-I. *Acta Crystallogr., Sect. C: Cryst. Struct. Commun.* **1976**, *32*, 62. (c) Ni, Y.; Fitzgerald, J. P.; Carroll, P.; Wayland, B. B. *Inorg. Chem.* **1994**, *33*, 2029−2035.

from planarity (σ) are small, but clearly dependent on the ligands bound to rhodium. In **2** and **4**, saddlelike conformations are adopted in which two opposite phenyl substituents are bent respectively upward and downward from the porphyrin plane while the two other phenyl substituents are not significantly distorted from the plane (Table 2). The porphyrin deformation is slightly more pronounced in **2** than in **4**. Disorder of the phenyl group at the *meso*-position C5 in **2** suggests that the porphyrin conformation may be variable, with this phenyl group adopting either a *syn*- or *anti*- conformation with respect to the phenyl group at the opposite *meso*-position as in a variety of (X)(I)Rh(TPP) complexes[33,34] and in (Me)Rh(DPP).[17] By contrast, porphyrin **5** shows an umbrella-like conformation, with the phenyl substituents on the *meso*-carbons bowed toward the methylide ligand. Similar distortions are observed in the monophosphine complex (PPh_3)(Cl)Rh(OEP)[9] and in CH_3Rh(F_{28}TPP).[5] The umbrella-like distortion appears to minimize steric interactions between the phosphine ligand and the phenyl substituents of the porphyrin core and arises where the ligand in the opposite axial position is relatively small. In **2** and **4**, in which the larger iodo ligand occupies the axial position opposite the phosphine, saddlelike conformations are observed. In the structures of **2**, **4**, and **5**, all phenyl substituents are twisted significantly from orthogonality to the porphyrin plane (Table 2). This twist is largest in **4** and appears to result from reduction of steric interactions between the phenyl rings and the phosphine ligands. In **2**, the Rh−OCH_3 and Rh−I bond distances of 2.210(6) and 2.5719(8) Å, respectively, compare well with values reported previously for analogous Rh(III) iodo porphyrins with alcohols in the sixth axial coordination site.[19,33]

Of particular interest are the structural features of the coordinated DPAP ligands. The Rh−P bond distances are significantly different in **4** and **5**, increasing by ca. 0.14 Å in **5** compared with **4**. This can be explained by a considerably larger *trans*-influence exerted by the methylide ligand compared with that for two phosphines *trans* to one another. The Rh−P bond distances in both **4** and **5** are longer than that reported for (PPh_3)(Cl)Rh(OEP) (2.306(3) Å)[9] and are also longer than in other rhodium phosphine complexes.[30,35] Introduction of the DPAP ligand in the sixth axial coordination site in **5** lengthens the bond to the *trans*-methylide carbon by ca. 0.09 Å compared with that in 5-coordinate **3**. The acetylenic groups in **4** and **5** deviate slightly from linearity, with bond angles 169.9(3)° in **4** (P1−C35≡C36), and 174(3)° and 172(4)° for the two orientations of P1−C58≡C59 in **5**.[25] The relative orientation of the DPAP unit with respect to the porphyrin core is similar in both **4** and **5**: to avoid steric interactions, the phenyl rings of the DPAP unit are located over the pyrrole groups. The two orientations of the disordered DPAP moiety in **5** are comparable, with the acetylenic groups located on either side of the *meso*-phenyl group at C10.

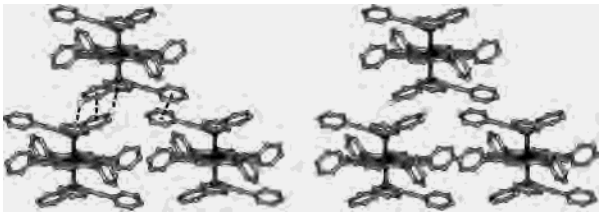

Figure 4. Stereo representation of part of the crystal packing in **4**. Solvent molecules, iodides, and hydrogen atoms are omitted, except for the *para*-hydrogen on the phosphine phenyl substituent, which is involved in the edge-to-face interaction in the crystal. The edge-to-face interaction and face-to-face offset stacking is indicated by dashed lines (- - -).

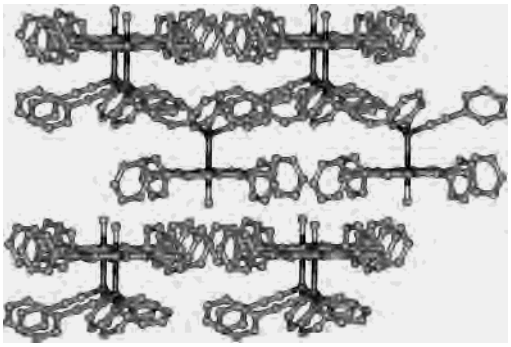

Figure 5. Ball and stick representation of part of the crystal packing in **5**. Hydrogen atoms have been omitted. Only one of the disordered geometries of the DPAP unit is shown.

Since there is rapid rotation about the Rh−P bond in solution, the positions of the DPAP moieties with respect to the porphyrin in the solid state are likely to be influenced by intermolecular interactions. In **4**, the complexes are arranged into layers (in the crystallographic *ab* plane) in which all porphyrin planes in a given layer are parallel. Each DPAP ligand interacts with the DPAP on two adjacent porphyrins within the layer (Figure 4). The interaction with the first porphyrin is reminiscent of the "phenyl embrace" commonly observed between PPh_3 groups,[36] in which the phenyl rings bound directly to P form mutual edge-to-face arrangements across a center of symmetry (interplane angle 44.2°, centroid-to-centroid distance 4.78 Å). The phenyl ring bound to the acetylenic group interacts in a face-to-face offset manner with the corresponding ring on a second porphyrin, with an interplane separation of 3.45 Å and a centroid-to-centroid distance of 3.69 Å. In **5**, the porphyrin complexes are arranged into "bilayers" in which the DPAP ligands interact at the center of the bilayer and the methylide ligands remain at the outside (Figure 5). The arrangement is clearly different from that in **4**, forming in this case a two-dimensional network of interactions.[37] The phenyl embrace exists between the phenyl groups bound directly to P, similar to that observed in **4**, although the rings adopt a significantly

(33) Simonato, J. P.; Pecaut, J.; Marchon, J. C. *Inorg. Chim. Acta* **2001**, *315*, 240.
(34) Jameson, G. B.; Collman, J. P.; Boulatov, R. *Acta Crystallogr., Sect. C: Cryst. Struct. Commun.* **2001**, *57*, 406.
(35) Lai, W.; Lau, M. K.; Chong, V.; Wong, W. T.; Leung, W. H.; Yu, N. T. *J. Organomet. Chem.* **2001**, *634*, 61.
(36) Dance, I.; Scudder, M. *Chem. Commun.* **1995**, 1039.
(37) The disordered description of the DPAP ligand arises from the two-dimensional network of the interactions between adjacent DPAP moieties within a given bilayer: those in adjacent porphyrins must adopt alternately the first and second orientation along one interaction direction (roughly along the [1$\bar{1}$0] direction), but the same orientation along the second interaction direction (roughly along [110]).

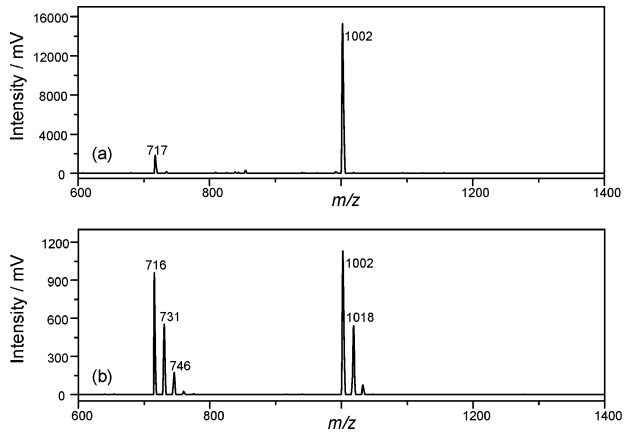

Figure 6. LDI-TOF mass spectra (a) of **4** and (b) of **5**, recorded in the positive ion mode as neat samples.

larger separation compared with **4** (interplane angle 68.6°, centroid-to-centroid distance 5.96 Å). This larger separation between the DPAP ligands accommodates additional edge-to-face interactions involving one of the phenyl groups at the *meso*-position of the second porphyrin (interplane angle 31.5°, centroid-to-centroid distance 4.95 Å). In addition, the phenyl ring attached to the acetylenic linkage interacts with the phenyl groups bound directly to P on two adjacent porphyrins, forming a 3-fold edge-to-face motif (Figure 5). Face-to-face interactions between phenyl rings are not observed in **5**.

LDI-TOF Mass Spectrometry. Mass spectrometric analyses of the complexes were performed using LDI-TOF MS without the addition of any matrix, which can interfere with the coordination of ligands.[38] Porphyrin **2** showed only a mass peak at *m*/*z* 716.4, which corresponds to the molecular ion with loss of iodide,[38] and represents the bare $[RhTPP]^{+\bullet}$ (calcd *m*/*z* 715.63). Similar behavior was reported when using LSI ionization.[14] Measurement of **3** showed three peaks in the molecular ion region, separated by 15 mass units. The peaks can be assigned to the molecular ion $[M]^{+\bullet}$ at *m*/*z* 730.7 (calcd *m*/*z* 730.66), the parent ion with loss of the methylide $[M - CH_3]^{+\bullet}$ at *m*/*z* 715.7 (corresponding to $[Rh(TPP)]^{+\bullet}$), and an additional peak at *m*/*z* 745.6, corresponding to the methylide adduct of **3** $[(Me)_2Rh(TPP)]^{+\bullet}$ (calcd *m*/*z* 745.69), arising from intermolecular methyl transfer. As can be seen in Figure 6b, the relative intensity is increasing with subsequent loss of the methyl groups. We have observed similar intramolecular transfers with iodo substituted porphyrins, and this was attributed to laser induced photolytic bond cleavage in the excited state.[38] Addition of a matrix such as hydroxy cinnamic acid, *p*-nitroaniline, or other porphyrins did not prevent the fragmentation of **3**.

The parent mass peak of **4** could not be detected, but loss of one DPAP ligand gave the mono-phosphine complex $[(DPAP)Rh(TPP)]^{+\bullet}$ at *m*/*z* = 1002.0 (calcd *m*/*z* 1001.93). When (DPAP)(Me)Rh(TPP) (**5**) was analyzed in the LDI-TOF MS, the molecular ion was detected at *m*/*z* 1018.2, together with a peak at *m*/*z* 1002.0 (loss of the methylide, see preceding description). The fragmentation in both **3** and **5** also affected the signal intensity. The observation that laser induced loss of the methylide can occur from the excited state in the gas phase is consistent with the reported photolysis of **3** to generate $Rh^{II}(TPP)$ in solution upon irradiation at 416 nm.[16] Dimerization, which often occurs with Rh(II)−porphyrins in solution,[3,13,39] was not observed in the gas phase.

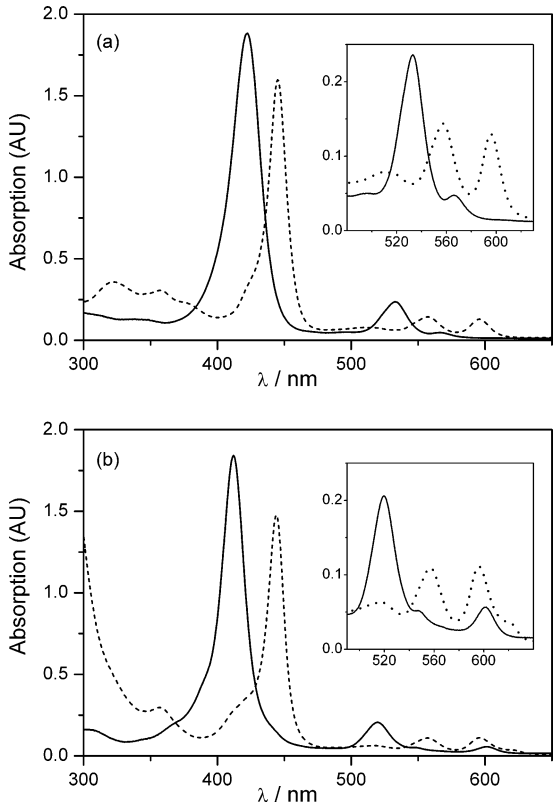

Figure 7. UV−vis spectra (a) of (MeOH)(I)Rh(TPP) (**2**) (—) and $[(DPAP)_2Rh(TPP)](I)$ (**4**) (- - -), and (b) of (Me)Rh(TPP) (**3**) (—) and (DPAP)(Me)Rh(TPP) (**5**) (- - -). The spectra are recorded in $CHCl_3$ at 298 K, $c = 10^{-5}$ M. The insets show the expanded part of the Q-band absorption region.

Table 3. Absorption Maxima of the UV−Vis Spectra of (MeOH)(I)Rh(TPP) (**2**), (Me)Rh(TPP) (**3**), $[(DPAP)_2Rh(TPP)](I)$ (**4**), (DPAP)(Me)Rh(TPP) (**5**), and (DPAP)(I)Rh(TPP) (**6**) in CH_2Cl_2, T = 298 K

	λ/nm (log ϵ)
(MeOH)(I)Rh(TPP) (**2**)	422 (5.27), 533 (4.37), 566 (3.68)
(Me)Rh(TPP) (**3**)	412 (5.29), 520 (4.34), 547 (3.73)
(DPAP)(I)Rh(TPP) (**6**)	437, 504[a]
$[(DPAP)_2Rh(TPP)](I)$ (**4**)	323 (4.63), 357 (4.56), 376 (shoulder), 445 (5.28), 557 (4.23), 596 (4.19)
(DPAP)(Me)Rh(TPP) (**5**)	356 (3.62), 418 (shoulder), 444 (5.22), 516 (3.85), 556 (4.09), 597 (4.10), 620 (3.62)

[a] λ values are calculated using a Gaussian peak deconvolution.

UV−Vis Spectroscopy. The UV−vis absorption spectra of **2**−**6**, measured in $CHCl_3$, are displayed in Figure 7, and the data are summarized in Table 3. Comparison with the electronic absorption data of **2**, preciously reported in a range of solvents,[15] confirms a significant solvatochromicity of the lower energy Q-band absorption, which is blue-shifted in

(38) Stulz, E.; Mak, C. C.; Sanders, J. K. M. *J. Chem. Soc., Dalton Trans.* **2001**, 604.

(39) Zhang, X. X.; Wayland, B. B. *Inorg. Chem.* **2000**, *39*, 5318.

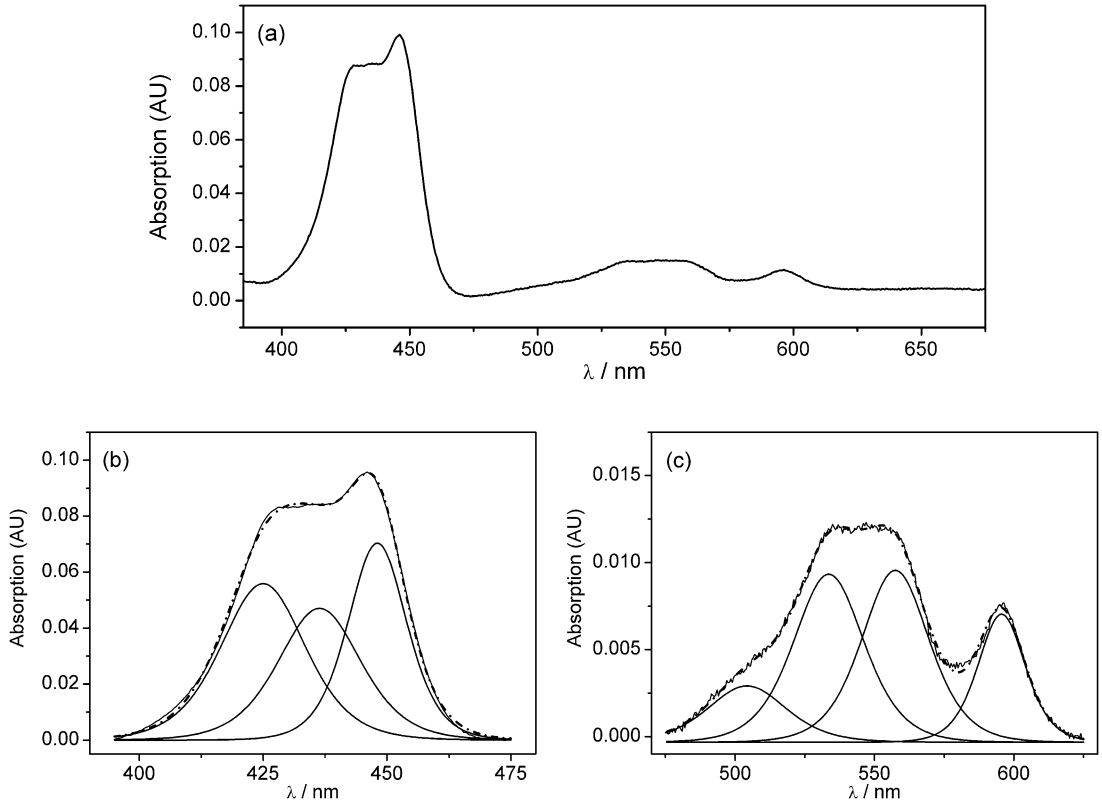

Figure 8. (a) Selected electronic spectrum of a mixture of **2**, **4**, and **6** obtained during the titration of **2** with **1**; [**2**] = 9.89×10^{-7} M, [**1**] = 1.38×10^{-6} M, 293 K. Peak deconvolutions (after baseline correction) are shown for the high energy part (b) and for the low energy part (c) of the spectrum; the broken lines show the calculated absorption based on the best fit.

$CHCl_3$ (566 nm) compared to the absorptions obtained in solvents with strong donor properties such as *n*-PrCN (570 nm), DMF (574 nm), or DMSO (578 nm). The absorption maxima found in **3** also match the reported data.[9,10,12,13,15,16]

Upon titration of **1** into a $CHCl_3$ solution of **2**, the intermediate complex (DPAP)(I)Rh(TPP) (**6**) can only be detected at low concentrations ([**2**] = 10^{-6} M). Since there is always a mixture of all three species **2**, **4**, and **6** present, the spectrum of **6** could not be measured in pure form. The absorption maxima of **6** were calculated using a Gaussian peak function to deconvolute the spectrum at two different rhodium-to-phosphine ratios. Figure 8 shows the results for one of the deconvolutions. The peaks found for **2** and **4** match the values obtained for the pure samples, confirming the validity of the method. The B-band absorption of **6** with a 437 nm is more red-shifted than the value previously observed for (PPh_3)(THF)Rh(TPP) (λ 425 nm)[13] but is close to that of (PPh_3)(Me)Rh(TPP) (λ 439 nm).[12] The red-shift of the B-band might indicate partial displacement of the weakly bound iodide.[15] The single Q-band absorption, which is normally found in mono-phosphine rhodium porphyrin complexes around 525−540 nm,[13] was located at 504 nm, which is a significant blue-shift, and displays the highest energy Q-band absorption for a phosphine rhodium complex so far. At higher concentrations of porphyrin ($>10^{-6}$ M), the titrations always yielded **4** directly. The final complex [($DPAP)_2$Rh(TPP)](I) (**4**) shows a bathochromic shift of the Soret band absorption of $\Delta\lambda$ = 23 nm compared to **2**, and the Q-bands are also red-shifted by 24 and 30 nm, respectively (Table 3). These values are very similar to those of the analogous PPh_3 and the more basic PPh_2Me and $PPhMe_2$ complexes. It seems that, in contrast to the mono-phosphine complex, the electronic spectra of the bis-phosphine complexes are relatively insensitive to the nature of the phosphine ligand; thus, the MO energy separations are affected minimally by changing the basicity of the ligand.

As was found for **6**, the electronic spectrum for (DPAP)(Me)Rh(TPP) (**5**) is very different from that for the corresponding PPh_3 complex. UV−vis measurements led Kadish et al.[12] to conclude loss of the methylide at low concentrations ($<10^{-5}$ M) to produce [($PPh_3)_2$RhTPP]$^+$, whereas at higher concentrations ($>10^{-3}$ M), the mono-complex (PPh_3)(Me)RhTPP is obtained.[40] However, upon titrating **1** into a solution of **3**, we always obtained a spectrum which essentially matched that of **4**, independently of the concentration of **3**, which ranged from 10^{-6} to 5×10^{-4} M. To determine whether this spectrum corresponds to that of **5** or **4**, we performed a ^{1}H NMR titration at 5×10^{-4} M porphyrin concentration. This experiment showed that, even when adding a large excess of ligand, the methylide remained bound to rhodium, as judged from the high field doublet resonance at ∼−6.5 ppm in the spectrum (data not shown). We therefore confidently assign the electronic spectrum measured as that of **5**. An additional low energy band at 620 nm is present in **5**, which is clearly missing in the spectrum of **4**. Some differences in the high energy part of

(40) We have been able to reproduce Kadish's unexpected results with PPh_3.

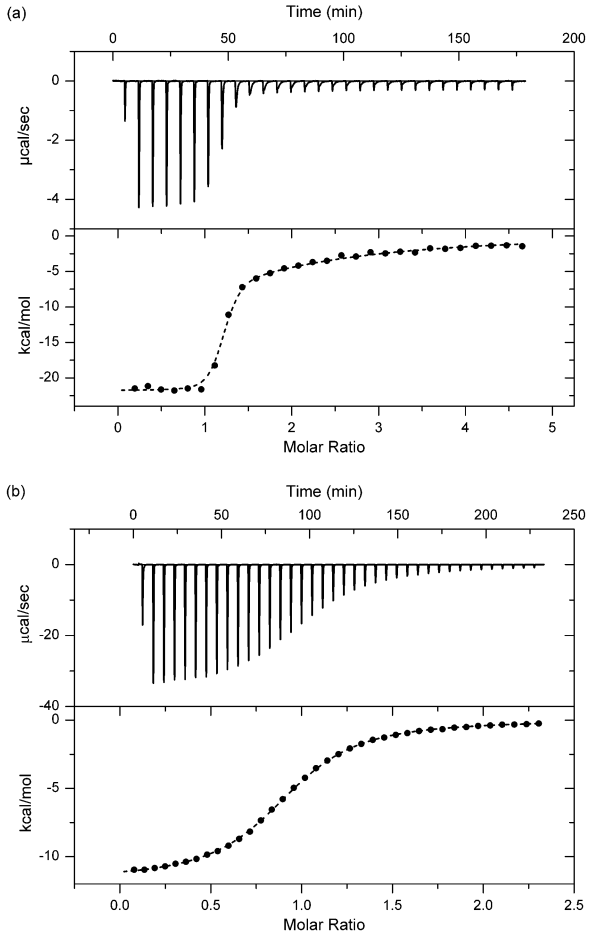

Figure 9. Isothermal titration calorimetry measurements (a) of **2** with **1**, and (b) of **3** with **1**. The upper parts of the figures display the measured heat effects, and the lower parts show the extracted enthalpy values. The dashed lines (- - -) represent the nonlinear fitting procedures to the data for the calculation of the thermodynamic parameters.

the spectra below 400 nm can be seen as well. Our UV−vis and NMR spectroscopic data indicate that the methylide is not displaced upon titrating **3** with **1** at any concentration. It seems also in this case that the MO energies of the monophosphine complex are highly sensitive to the nature of the phosphorus ligand. Using a wider range of different σ-donor and π-acceptor phosphines or phosphonates should therefore lead to very different electronic properties of the complexes obtained.

Isothermal Titration Calorimetry. Thermodynamic data of ligand binding to metalloporphyrins are relatively scarce. Solvent effects on the binding of pyridine to zinc porphyrins have been described.[41] Also, the values for the binding of PPh_3 to (Cl)Rh(OEP), obtained by variable temperature equilibrium measurements, have been reported.[9] In order to gain insight into the thermodynamics of the binding of ligand **1** to rhodium(III) porphyrins, we have performed isothermal titration calorimetry (ITC) with both **2** and **3** at 298 K (Figure 9).

(41) (a) Zielenkiewicz, W.; Lebedeva, N. S.; Antina, E. V.; Vyugin, A. I.; Kaminski, M. *J. Solution Chem.* **1998**, *27*, 879. (b) Zielenkiewicz, W.; Lebedeva, N. S.; Kaminski, M.; Antina, E. V.; Vyugin, A. I. *J. Therm. Anal.* **1999**, *58*, 741.

Table 4. Thermodynamic Data Obtained from the Isothermal Calorimetry Titrations of Reactions 1, 2 and 3[a]

	$\Delta G°$/ kJ mol^{-1}	$\Delta H°$/ kJ mol^{-1}	$T\Delta S°$/ kJ mol^{-1}	K_a/M^{-1}
1, (DPAP)(I)Rh(TPP) (**6**)	−42.7	−90.4	−47.7	3.0 (±0.6) × 10^7
2, [(DPAP)$_2$Rh(TPP)](I) (**4**)	−25.1	−54.0	−28.8	4.6 (±0.6) × 10^4
3, (DPAP)(Me)Rh(TPP) (**5**)	−24.6	−54.0	−29.3	2.1 (±0.03) × 10^4

[a] See text; $CHCl_3$, T = 298 K.

The thermodynamic data, summarized in Table 4, show that complexation of **1** to any of the rhodium porphyrins is exothermic, and all binding events are enthalpy driven. The first binding to (MeOH)(I)Rh(TPP) (**2**) according to reaction 1, which has a Gibbs standard free energy change of $\Delta G_1° = -42.7$ kJ mol^{-1}, shows the largest change both in enthalpy ($\Delta H_1° = -90.4$ kJ mol^{-1}) and in entropy ($T\Delta S_1° = -47.7$ kJ mol^{-1}). These values are much larger than those obtained for the binding of pyridine to zinc tetraphenyl porphyrin in chloroform ($\Delta G_{Py}° = -20.6$ kJ mol^{-1}, $\Delta H_{Py}° = -35.8$ kJ mol^{-1}, $T\Delta S_{Py}° = -15.2$ kJ mol^{-1}).[41] Reaction 1 involves displacement of a weakly bound solvate molecule (methanol) by **1**, and the large value for $\Delta H_1°$ indicates a high Rh−P bond energy in **6**. The relatively large entropic contribution might arise from much stronger solvation of the released polar methanol by $CHCl_3$ compared to **1**. Reactions 2 and 3 show almost identical Gibbs free energy changes: $\Delta G_2° = -25.1$ kJ mol^{-1} and $\Delta G_3° = -24.6$ kJ mol^{-1}, respectively. The enthalpy change $\Delta H_{2,3}°$ is −54.0 kJ mol^{-1} for both reactions, and the change in entropy $T\Delta S_2°$ and $T\Delta S_3°$ differ only by 0.5 kJ mol^{-1}. All values for reactions 2 and 3 are about 0.59 that of the first binding of **1** to **2**.

$$\text{DPAP (}\mathbf{1}\text{)} + \text{(MeOH)(I)Rh(TPP) (}\mathbf{2}\text{)} \rightleftarrows \text{(DPAP)(I)Rh(TPP) (}\mathbf{6}\text{)} + \text{MeOH} \quad K_{a1} \quad (1)$$

$$\text{DPAP (}\mathbf{1}\text{)} + \text{(DPAP)(I)Rh(TPP)} \rightleftarrows \text{[(DPAP)}_2\text{Rh(TPP)](I) (}\mathbf{4}\text{)} \quad K_{a2} \quad (2)$$

$$\text{DPAP (}\mathbf{1}\text{)} + \text{(Me)Rh(TPP) (}\mathbf{3}\text{)} \rightleftarrows \text{(DPAP)(Me)Rh(TPP) (}\mathbf{5}\text{)} \quad K_{a3} \quad (3)$$

The enthalpy change for reaction 2 is larger than for the displacement of chloride from (PPh_3)(Cl)Rh(OEP) to form $[(PPh_3)_2$Rh(OEP)](Cl), where a value of $\Delta H_{PPh3}° = -32.6$ kJ mol^{-1} was determined in CH_2Cl_2.[9] The entropy change $T\Delta S_{PPh3}°$ for the displacement of chloride by PPh_3 is −43.4 kJ mol^{-1} (calcd at 298 K) and is considerably more unfavorable than the entropy change associated with the displacement of iodide in our system, which could be due to solvation effects of the different ions released in the reactions. In fact, the displacement of chloride by PPh_3 is overall an unfavorable reaction ($\Delta G_{PPh3}° = 10.8$ kJ mol^{-1}, $K_{assoc} = 0.0174$).[9]

In reaction 3, no bonds are being broken, and to a first approximation, the $\Delta H_3°$ value can be regarded as reflecting the Rh−P bond energy in **5**. The value of $\Delta H_3° = -54.0$ kJ mol^{-1} is in the range of the reaction enthalpies found for displacement of cyclooctene by PPh_3 in other rhodium complexes ($\Delta H_{PPh3}° = -30$ to -45 kJ mol^{-1}).[30] Compared

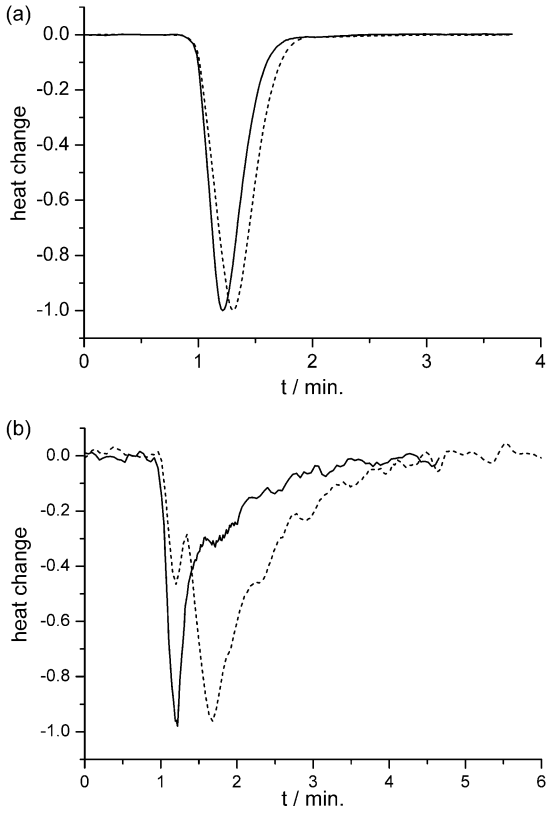

Figure 10. Overlay of the ITC profiles recorded during titration of the porphyrins with DPAP (**1**) in $CHCl_3$. The peaks are normalized to the same height. (a) (—) **2** with **1**, (- - -) **3** with **1**, (b) (—) **6** with **1**, (- - -) **6** with **1** in the presence of 5 equiv of iodide.

to the binding of pyridine to Zn(TPP) in $CHCl_3$,[41] which is similar in that no ligand displacement occurs, the bond energy in **5** is stronger by $\Delta\Delta H° = -18.2$ kJ mol^{-1}, but the larger entropy cost of $\Delta\Delta S° = 14.1$ kJ mol^{-1} might be due to the loss in rotational freedom of the substituents on the phosphorus, caused by steric interactions with the porphyrin core. In addition, desolvation must be taken into account. For reaction 3, almost the same change in enthalpy is observed as for reaction 2, and this could be explained by two factors: (i) the iodide is only weakly bound, so that displacement does not require significant enthalpy contributions, and (ii) the axially bound phosphine has an overall similar electronic *trans*-influence as the σ-bonded methyl group.

Figure 10 shows the overlay of some of the injections recorded upon formation of **4**, **5**, and **6**. The almost identical profiles for the formation of **5** and **6** (Figure 10a) indicate that the MeOH is only very weakly bound and is rapidly displaced or even already dissociated in this concentration range. On the other hand, the formation of **4** consists of two different processes, as can be seen from the shape of the recorded peak in Figure 10b (—). After an initial rapid reaction, the peak shape changes, and the process follows a much slower pathway. Addition of 5 equiv of iodide (as *tert*-butylammonium salt) changes the heat emission profile, and the two processes become clearly visible [Figure 10b (- - -)]. A first small and sharp peak, identical in shape to the ones obtained for reactions 1 and 3, is followed by a second, broad peak of much larger intensity, and showing a maximum heat effect ca. 1.7 min after initial mixing. The heat effect of the second process, which dominates in the presence of excess iodide, arises from reaction 2. This indicates that, at concentrations in the submillimolar range, the iodide is partially displaced, and **6** actually exists largely as a contact ion pair $[(DPAP)Rh(TPP)]^+\cdots I^-$. The coordination of **1** to the 5-coordinate $[(DPAP)Rh(TPP)]^+$ is rapid, in contrast to the displacement of iodide in reaction 2. The rate determining step in reaction 2 therefore seems to be dissociation of the iodide.

For the binding of **1** to **2**, the data were fitted using a model with two independent binding events, and the stoichiometries were in good agreement with a 1:1 stoichiometry for each binding site. For the binding of **1** to **3**, the fitting procedure was performed using a single binding model, again in agreement with a stoichiometry of 1:1. No displacement of the methyl group was observed. The thus obtained values for K_{assoc} agree well with the values calculated from UV−vis titrations (data not shown). Clearly, formation of **6** shows the highest thermodynamic stability with $K_{a1} = 3.0\ (\pm 0.6) \times 10^7$ M^{-1}. The second binding of **1** to **4** is less favorable by a factor of about 1000 [$K_{a2} = 4.6\ (\pm 0.6) \times 10^4$ M^{-1}]. A similar decrease in binding strength has been reported for the complexation of PPh_3 to $(O_2)Rh(TPP)$.[10] Since the basicity of iodide ($pK_a = -11$) is much lower than that of **1** ($pK_a = 1.04$),[25] the much weaker second binding is due to the much stronger σ/π-interactions of the phosphine ligand compared to iodide. Phosphorus ligands are expected to have a strong *trans*-influence,[35] which is expressed in the thermodynamic parameters. However, a large *trans*-effect, which would affect the kinetics of the displacement reactions, does not seem to be the case, because the ligand exchange of iodide with **1** is relatively slow.

$K_{a3} = 2.1\ (\pm 0.03) \times 10^4$ M^{-1} is in the same order of magnitude as K_{a2}. This value is about 10 times larger than the binding of PPh_3 to **3** ($K_{assoc} = 3.9 \times 10^3$ M^{-1}).[12] Since PPh_3 is a stronger base ($pK_a = 2.73$)[42] than **1**, the weaker binding of PPh_3 is most probably due to steric effects. We have already observed an analogous difference in the binding of PPh_3 and **1** to ruthenium porphyrins.[25] Strong binding of a sixth ligand was not expected, since alkyl rhodium porphyrins usually do not have additional solvent molecules such as alcohols or ethers attached, both in solution and in the solid state, contrary to the halide complexes. The σ-bonded methylide does not have any significant π-acceptor properties, and the high basicity ($pK_a \sim 50$) drastically increases the electron density on the metal, thus reducing the electrophilicity of the metal, hence the much lower K_{a3} value.

Conclusions

We have presented the analytical data of new phosphine rhodium porphyrin complexes, including spectroscopic studies (UV−vis, ^{1}H NMR, and ^{31}P NMR), mass spectrometry, thermodynamic analysis, and the solid-state structures of all

(42) Henderson, W. A.; Streuli, C. A. *J. Am. Chem. Soc.* **1960**, *82*, 5791.

complexes. The spectroscopic results presented here show that the properties of phosphine (P) complexes (P)(X)Rh^{III}(TPP) are sensitive to the nature of the axial *trans*-ligand X, where X = I, Me, or P. The mono-complexes of DPAP (**1**) display especially large differences in the thermodynamic parameters and in the electronics of the porphyrin, i.e., in the UV−vis and ^{31}P NMR spectra, depending on whether the *trans*-ligand is iodide as in **6**, or methylide as in **5**. In the former case, binding is strong and is accompanied by large changes in enthalpy and entropy; in the latter case, binding is relatively weak, and the thermodynamic changes are significantly smaller. The nature of the phosphine ligands also seems to have a large influence on the electronics of the complex formed. Even though the absorption spectrum of **5** resembles the spectrum of **4** very closely, loss of the σ-bonded methyl ligand is not observed, contrary to what was found with the slightly more basic PPh_3 as ligand.[12]

For the bis-phosphine complex **4**, the electronic spectrum obtained is very similar to those reported with other phosphine ligands.[8,11−13,15] The relative energies in the bis-phosphine complexes therefore do not seem to be very sensitive to the nature of the phosphorus ligand. The phosphorus as *trans*-ligand weakens the second binding considerably. The spectroscopic and thermodynamic data suggest that **1** and Me have an almost identical *trans*-influence on the opposite axial ligand, but these arise from very different σ-donor and π-acceptor properties. The electronic spectra are strikingly similar, despite the large differences of the absorption spectra of the free porphyrins **2** and **3**. ^{31}P NMR spectroscopy has shown to be very sensitive to the nature of the *trans*-ligand: in **4** and **6**, the resonances are sharp and downfield shifted compared to the free phosphine. Since both complexes are almost isochronous, the Rh−P coupling constants can be used to distinguish the two complexes. In the case of a σ-bonded alkyl group as sixth ligand, the ^{31}P NMR spectrum displays a broad and only marginally shifted resonance for the bound phosphine. Also, no $^1J_{Rh,P}$ coupling could be observed. This behavior can be explained by a dynamic ligand exchange of unbound and bound species.

A recent density functional computational study found[43] that metal−phosphine bond energies cannot be regarded as intrinsic, universal, or transferable properties, and the synergy between σ-donor and π-acceptor ligands is pivotal in the interpretation of bond enthalpies. Our thermodynamic data show that very similar values can be observed when ligands exhibiting large differences in σ/π-properties are *trans* to each other. Overall, the *trans*-influence of the σ-bonded methyl group is comparable to **1**, but in the former, it is due to strong σ-donation, whereas in the latter the π-acceptor properties seem to play an important role.

Since the phosphine ligand used in these studies serves us as a model for our phosphine substituted porphyrins, the results discussed here let us predict that incorporating rhodium porphyrins in our supramolecular arrays will lead to complexes exhibiting attractive physicochemical properties. The binding constants of alkynyl phosphines to Rh(III) porphyrins are high enough to be useful in the construction of a stable supramolecular structure (Chart 1). Both axial sites on the porphyrin can be used for complexation; however, the sixth coordination site can be blocked by introducing a σ-bonded methyl group, allowing the selective formation of mono-phosphine complexes without strongly affecting the electronic properties. The results show that **1** is a very versatile ligand which forms more stable complexes with rhodium(III) porphyrins than PPh_3 and is a good model for studying phosphine−rhodium interactions in larger arrays.

Acknowledgment. Financial support from the Swiss National Science Foundation (E.S.), from the Royal Society (S.O.), and from the EPSRC (E.S., S.M.S., and A.D.B.) is gratefully acknowledged.

Supporting Information Available: X-ray crystallographic tables for structures **2**, **3**, **4**, and **5** (atomic coordinates, bonds lengths and angles, anisotropic thermal factors, hydrogen atom positions as CIF files). This material is available free of charge via the Internet at http://pubs.acs.org.

IC026257A

(43) Landis, C. R.; Feldgus, S.; Uddin, J.; Wozniak, C. E.; Moloy, K. G. *Organometallics* **2000**, *19*, 4878.